Available online at www.sciencedirect.com
SCIENCE DIRECT®
Catalysis Today 91–92 (2004) 91–97
CATALYSIS TODAY
www.elsevier.com/locate/cattod

Carbon nanotubes as nanosized reactor for the selective oxidation of H_2S into elemental sulfur

Jean-Mario Nhut, Patrick Nguyen, Cuong Pham-Huu*, Nicolas Keller, Marc-Jacques Ledoux

Laboratoire des Matériaux, Surfaces et Procédés pour la Catalyse, UMR 7515 du CNRS, ECPM, ULP, ELCASS (European Laboratory for Catalysis and Surface Sciences), 25 rue Becquerel, 67037 Strasbourg Cedex 2, France

Abstract

Selective oxidation of H_2S into elemental sulfur at near-ambient temperature have been carried out over NiS_2 nanoparticles encapsulated inside multi-walled carbon nanotubes (MWNTs). The high capacity of solid sulfur storage on the MWNT-based catalyst compared to that of macroscopic SiC grains was thus attributed to the large void volume outside the MWNTs available for the sulfur storage when compared to the void volume outside the SiC grains.

Keywords: Carbon nanotubes; Elemental sulfur; Atomic absorption spectroscopy

1. Introduction

Carbon nanostructures, nanotubes and nanofibers have received increasing scientific interest since the discovery of nanotubes in 1991 by Iijima as by-products of the arc-discharge synthese [1]. These nanostructured materials exhibit extraordinary mechanical strength, electrical and thermal properties which render them attractive for several potential applications and has induced a large research effort in the last decade [2–4]. Among all the potential applications cited the use of carbon nanotubes and/or nanofibers as catalyst support seems to be the most promising [5–12]. The high aspect, i.e. length-to-diameter, ratio confers on them a high external surface area which significantly reduces the problems of mass transfer and allows obtention of high catalytic performances compared to conventional solid carriers. In addition, the complete absence of microporosity in the carbon nanotubes also makes them very attractive compared to the traditional activated charcoal support in which the large number of micropores greatly increases the diffusion phenomena, especially in liquid phase processes. Finally, it should be noted that the tubular morphology of the carbon nanotubes could also lead to a peculiar reactivity of gaseous or liquid reactants when passing through the tubules, e.g. a confinement effect [13].

Hydrogen sulfide, H_2S, is released from different sources, i.e. natural gas plant and refinery. Due to its high toxicity, H_2S must be removed as much as possible before releasing the off-gas into the atmosphere. The general trend is to selectively transform the H_2S into elemental sulfur using the equilibrated Claus process: $2H_2S + SO_2 \leftrightarrow (3/n)S_n + 2H_2O$ [14]. However, the thermodynamic limitations of the Claus equilibrium reaction fix the maximum conversion level at about 97%. This has led to the development of new processes to deal with the Claus tail-gas, based on the direct catalytic oxidation of remaining traces of H_2S (=1 vol.%) by oxygen into elemental sulfur, in order to meet ever stricter legislation requirements. Details concerning all these processes were recently summarized in a series of reviews published in the literature, but the catalysts, which are the core of the process, still need to be improved [15–18]. Recently, it has been reported that silicon carbide (SiC)-based catalysts exhibited high catalytic performances for this reaction either in a discontinuous mode (reaction temperature = 100 °C) or in a continuous mode (reaction temperature = 180 °C) [19–21]. In discontinuous mode, SiC-based catalysts allowed transformation of the totality of the inlet H_2S (ca. 2000 ppm) into elemental sulfur at reaction temperatures

* Corresponding author. Tel.: +33-390-2426-75; fax: +33-390-2426-74.
E-mail address: cuong.lcmc@ecpm.u-strasbg.fr (C. Pham-Huu).

0920-5861/$ – see front matter © 2004 Elsevier B.V. All rights reserved.
doi:10.1016/j.cattod.2004.03.015

ranging between 40 and 100 °C with a sulfur yield approaching 100% [19,20]. In order to reduce the size of the reactor, the catalyst should be able to work at a high space velocity. However, at a space velocity higher than 0.007 h^{-1} a significant drop in desulfurization activity was observed, attributed to the low adsorption rate of the reactant. In addition, the catalyst rapidly deactivated as a function of time on stream due to the blockade of the active sites by the solid sulfur deposit. It is of interest to find a new catalytic system which allows the selective oxidation of H_2S at a space velocity as high as possible, without an excessive loss of conversion and with a limited deactivation with time on stream.

Multi-walled carbon nanotubes (MWNTs) exhibit several advantages for use as catalyst support with respect to the H_2S selective oxidation process: (i) the chemical inertness of the support which avoids sulfation problems as usually encountered with alumina-based supports, and (ii) the absence of bottled pores, which can artificially modify the reactant and product residence time, and in turn decrease the process selectivity. The small size of the nanostructured carbon materials also significantly contributes to the final catalytic performance of the system due to the fact that catalytic reactions are governed by the phenomena of mass and heat transport between the catalyst particles and the reactants. It is also expected that the tubular morphology and the high aspect ratio of MWNTs could induce a confinement effect on the gas or liquid trapped inside their tubules, leading to specific physicochemical behaviors when compared to that observed on the bulk material. Several reports have recently dealt with the behavior of fluids trapped inside these high aspect ratio tubular materials [22-25]. The confinement effect inside MWNTs recently allowed the direct synthesis of magnetically active $CoFe_2O_4$ nanowires encapsulated inside MWNTs at the low temperature of 100 °C [25]. The aim of the present article is to report the use of an NiS_2 catalyst encapsulated inside MWNTs for the selective oxidation by oxygen of trace amounts of H_2S in the Claus tail-gas at the low reaction temperature of 60 °C. The catalytic performances of the NiS_2/MWNTs are also compared with those obtained on the NiS_2/β-SiC catalyst under similar conditions.

2. Experimental

2.1. Materials

MWNTs with a mean outer diameter of 100 nm, a mean inner diameter of 60 nm and lengths up to a dozen micrometers (average aspect ratio of ca. 30) were supplied by Sciences Inc. (Ohio, USA) and used as received. A large number of tubes were hollow from tip to tail even if some bamboo-like or closed tubes were also observed. The tubes were relatively straight with few defects according to the microscopy images. The material had a specific surface area measured by N_2 adsorption at liquid nitrogen temperature of 18 $m^2\,g^{-1}$ and a mesoporous system. No trace of microporosity was observed.

2.2. Characterization techniques

The metal loading was analyzed by atomic absorption spectroscopy (AAS) performed at the Service Central d'Analyse of the CNRS, Vernaison, France. Scanning electron microscopy (SEM) was carried out on a field emission scanning microscope model Jeol JSM-6700F working under low accelerating voltage, 3–15 kV, and allowing microstructural investigations down to a few nanometers. Transmission electron microscopy (TEM) and energy dispersive spectroscopy (EDS) microanalysis were used to provide information on the location and dispersion of the active phase, together with its particle size, morphology and composition. TEM and EDS were carried out in a Topcon Model EM200B operating at 200 kV, equipped with beryllium window detectors, with a point-to-point resolution of 0.17 nm.

2.3. Catalyst preparation and catalytic application

The nickel was introduced using an incipient wetness impregnation of the MWNTs by an ethanolic solution of nickel nitrate with a theoretical concentration of 5 wt.%. The wet solid was dried at 100 °C for 2 h and then calcined in air at 300 °C for 2 h in order to transform the salt precursor into its corresponding oxide. The reaction was carried out in a glass tubular microreactor (length: 800 mm; diameter: 25 mm) with the reactant mixture passing downward through the catalyst bed. The NiO phase was then sulfided in situ at 300 °C. The formation of the NiS_2 phase was confirmed by X-ray diffraction characterization. Details concerning the preparation and extensive characterization of the NiS_2–5% SiC reference catalyst have been already reported in previous publications [19,20,26]. After sulfidation, the reactor temperature was decreased to 60 °C under a helium flow and the reaction was started. The reaction conditions were as follows: H_2S, 2000 ppm; O_2, 3200 ppm; H_2O, 30 vol.% and balance helium, which are typically the industrial working concentrations in a discontinuous mode. At the reaction temperature, i.e. 60 °C, most of the steam condensed at the head of the reactor and the reaction was carried out in a trickle-bed mode. In order to avoid condensation, all the exit lines were maintained at 120 °C with heating tapes. The analysis of the inlet and outlet gas was performed on-line (six-port calibrated loop of 500 μl) using a Varian CX-3400 gas chromatograph equipped with a Chrompack JSQ capillary column allowing the detection of O_2, H_2S, H_2O and SO_2.

3. Results and discussion

The SEM image of the starting NiS_2 catalyst encapsulated inside the MWNT tubules is displayed in Fig. 1A. The NiS_2 particles located inside the MWNTs can be clearly

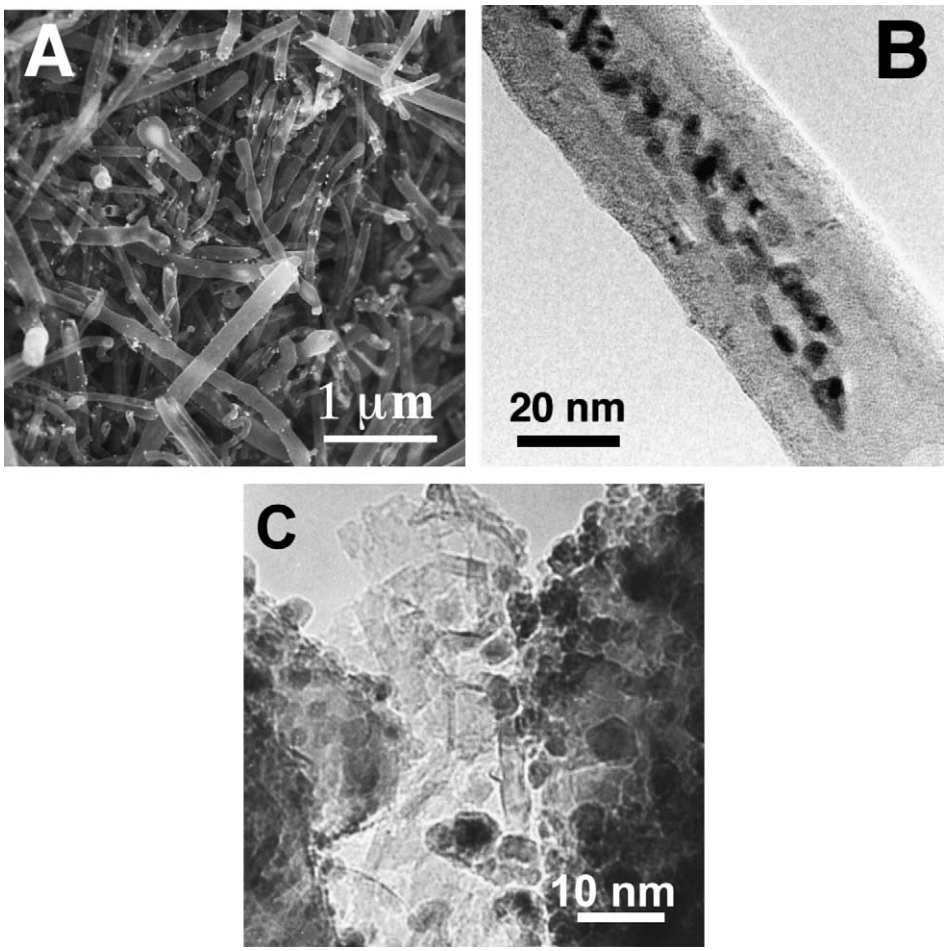

Fig. 1. (A) SEM and (B) TEM micrographs of the NiS_2/MWNTs catalyst. The TEM image shows an MWNT with the inner wall decorated with highly faceted nickel particles, probably due to the interaction between the surrounding wall of the nanotube and the nickel precursor. (C) TEM micrograph of the SiC-supported nickel catalyst showing a round-shaped morphology.

visualized using a high accelerated voltage. Some small NiS_2 particles were also visible on the outer surface of the carbon nanotube support. The NiS_2 location and microstructure were characterized using the TEM technique with a high lateral resolution. According to the TEM image (Fig. 1B), the quasi-totality of the NiS_2 particles was located within the MWNTs with an average particle size of about few nanometers. It should be noted that the NiS_2 particle formed inside the MWNTs were faceted, i.e. rectangular morphology or round shaped with a peculiar orientation with respect to the tube axis, which was completely different to that observed on traditional supports, i.e. round-shaped morphology with a random orientation [19]. The peculiar NiS_2 morphology observed could be attributed to the influence of the carbon wall during the thermal treatment processes, which could induce the anisotropy morphology observed by TEM. It is expected that depending on the metal–support interactions, the final metal particle size can be significantly altered from a round shape to highly faceted one. The facetage observed on the nickel active phase could be also the origin of the high catalytic activity observed below due to the different adsorption properties of the nickel sulfide faces. Such a specific morphology was already reported by Baker and co-workers, who observed flat and hexagonal nickel particles on carbon nanostructures compared to round-shaped particles on an alumina support [6]. TEM image of the NiS_2/SiC catalyst is displayed in Fig. 1C and clearly shows a round-shaped morphology for the nickel particles, compared to the rectangular one observed on the MWNTs.

The catalytic results obtained at 60 °C and with a weight hourly space velocity (WHSV) of 0.03 h^{-1} over the different catalysts are displayed in Fig. 2. It should be noted that the WHSV was deliberately chosen to be about three times higher than that usually encountered in a commercial plant for this reaction in order to verify the resistance behavior of the catalysts tested. At the reaction temperature of 60 °C, a selectivity towards elemental sulfur of 100% was obtained, no trace of SO_2 by-product having ever been observed, in good agreement with our previous work and the literature [20,27,28]. The catalytic performances were thus only based on H_2S conversion and resistance to solid sulfur deposition

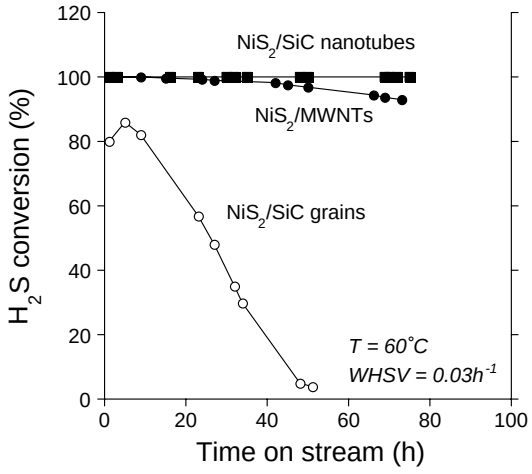

Fig. 2. Desulfurization performance of the NiS_2/MWNTs, NiS_2/SiC nanotubes and NiS_2/β-SiC (grains) catalysts at 60 °C in a trickle-bed mode. Reaction conditions—reaction temperature: 60 °C; H_2S: 2000 vol. ppm; O_2: 3200 vol. ppm; H_2O: 30 vol.% and balance He; WHSV = 0.03 h^{-1}.

onto the catalyst. The desulfurization activity obtained on the NiS_2/SiC nanotubes was also included in the figure for comparison.

At the WHSV of 0.03 h^{-1} the grain size SiC-based catalyst underwent rapid deactivation within a few hours (Fig. 2). The catalyst showed a short activation period, attributed to the time required by the NiS_2 phase to be superficially transformed into a new oxysulfide active phase, formed by the oxygen–sulfur atom exchange [20,26]. The deactivation observed was attributed to the high space velocity, i.e. H_2S molecules could not be adsorbed on the active sites to further react with oxygen, and to the blockade of the active sites by the solid sulfur deposit. Previous work at a lower WHSV has shown the role of condensed water in a trickled-bed mode, acting as a conveyor belt on the catalyst surface for the continuous removal of the solid sulfur from the active sites [20,29,30]. This transport phenomenon by water seemed to be insufficient at a high WHSV and thus, the solid sulfur formed would remain on the active sites, resulting in catalyst deactivation by encapsulation. Similar catalytic behavior was also observed on the alumina-based catalyst, which displayed a conversion of about 10% after only a few hours on stream [30]. In contrast, the MWNT-based catalyst exhibited an exceptionally high desulfurization activity, and after 70 h of test a conversion of the inlet $H_2S > 90\%$ was still observed. The solid sulfur deposited on the NiS_2/MWNT catalyst was about 180 wt.%. The deactivation slope observed on the catalyst after 50 h on stream was attributed to a partial blockage of the NiS_2 sites by the solid sulfur formed during the reaction. The mode of sulfur deposition with respect to the active sites was expected to be strongly influenced by the presence of steam, i.e. 30 vol.%, in the reactant feed. It is significant to note that despite the nanometer size of the catalyst and the large amount of solid sulfur deposited on the catalyst, almost no pressure drop across the

Table 1
Characteristics of the NiS_2/MWNTs and NiS_2/SiC catalysts at the end of the catalytic run

	NiS_2/MWNTs	NiS_2/SiC
Time on stream (h)	50	70
H_2S conversion (%)	>90	<5
Solid sulfur loading (wt.%)	180	50
S_{BET} (S_{BET} of the fresh catalyst) ($m^2\ g^{-1}$)	6 (18)	5 (24)

catalyst bed was observed. Table 1 summarizes the characteristics of the used catalysts after the catalytic runs. It was worth noting that the NiS_2/MWNTs kept part of its starting specific surface area, with a slight decrease from 18 $m^2\ g^{-1}$ down to 6 $m^2\ g^{-1}$ when the sulfur loading was greater than 180 wt.% and the H_2S conversion greater than 90%, whereas the surface area of the used and quasi-totally non-active NiS_2/SiC catalyst drastically decreased from 24 to 5 $m^2\ g^{-1}$ with a solid sulfur loading of 50 wt.%. This led to the idea that a peculiar mode of sulfur removal from the active sites and deposition on specific storage zones of the material occurred on the NiS_2/MWNTs catalyst as already found on the NiS_2/SiC catalyst [19,20,26]. The SiC nanotubes-based catalyst exhibits a highest desulfurization activity. However, the MWNTs-based catalyst was preferred owing to its simpler synthesis procedure when compared to that encountered with the SiC nanotubes, i.e. high-temperature gas–solid reaction between the MWNT and the SiO vapor.

Several non-exclusive hypotheses could be put forward to explain the high catalytic performances observed on the NiS_2/MWNTs catalyst compared to its NiS_2/SiC analogue:

(i) The small size of the support and the complete absence of bottled pores provided a high contact surface between the gaseous reactants and the catalyst, with minimum diffusional phenomena when compared to those encountered in traditional solids with bottled pores. In this latter case, competitive diffusion and back-diffusion between the gaseous reactants and the products could lead to a decrease in the catalytic activity.

(ii) The occurrence of a confinement effect inside the MWNTs, which would be linked to the peculiar location of the NiS_2 active phase inside the tubes. Such a concept has already been proposed to explain the high performances obtained on SiC nanotube-based catalysts for the same reaction [12]. It is based on the differentiation between the reaction conditions, inside and outside the MWNTs. According to the already known positive reaction order relative to H_2S, the increase in WHSV would be compensated by an increase in the H_2S partial pressure on the catalytic sites, in order to maintain the initial reaction rate. This concept would be based on the increase in the H_2S partial pressure inside the MWNTs, probably by microcapillarity due to the high dipolar moment of H_2S molecules. The apparent macroscopic H_2S partial

pressure, outside the tubes, would remain unchanged, while the microscopic or nanoscopic partial pressure would significantly increase inside the tubes. This modification of the reactant partial pressure probably occurred during the flow through the tube.

(iii) The highly faceted morphology or the peculiar exposed surface of the nickel sulfide particles inside the MWNTs could result in specific adsorption properties, and thus a different activity compared to round-shaped particles. Such an explanation has already been put forward by Baker and co-workers, who have attributed the peculiar activity obtained on graphite nanofiber-supported nickel catalysts for the butadiene or crotonaldehyde hydrogenation to a specific morphology adopted by the nickel phase [6].

The MWNT-based catalyst also exhibited an exceptionally high resistance towards deactivation by solid sulfur encapsulation as almost no activity loss was observed, even with a solid sulfur deposit greater than 180 wt.%. Taking into account the specific surface area of the starting support ($20\,m^2\,g^{-1}$) and considering that the cross-section is the lowest surface occupied by a sulfur molecule, i.e. $1.5\,nm^2$ per S_8 molecule, sulfur being generally present as S_8 in these conditions of temperature and pressure [29,30], it is expected that the complete coverage of the catalyst was attained with a solid sulfur concentration of about 4 wt.%. Such a coverage would induce the complete deactivation of the catalyst by encapsulation of the active sites by solid sulfur. The high desulfurization activity observed even when the sulfur loading on the catalyst surface reached more than 180 wt.% could be attributed to a specific and discrete sulfur deposition with respect to the active sites. The hypothesis about the heterogeneous deposition mode of sulfur was explained by the presence of a large excess of condensed water inside the MWNTs, which induced a continuous washing of sulfur from the active sites. The solid sulfur formed on the active sites was slowly moved by water from the hydrophilic inner wall of the support, and subsequently deposited onto the outer wall of the support which is hydrophobic in nature. The hydrophilic nature of the inner channel was expected to be due to the presence of a relatively large number of defects which could induce the formation of oxygenate groups with high affinity towards water. In the absence of steam, the desulfurization activity was extremely low, i.e. 10%, which indicate that the presence of steam was necessary for the sulfur removal from the active sites.

The hypothesis advanced above on the role of the duality character of the carbon nanotube surface was confirmed by SEM images taken on the spent catalyst (Fig. 3). Solid sulfur was observed randomly on the outer surface of the catalyst as relatively large spheres. Sometimes, several tubes were wrapped by a large sphere of solid sulfur. It should be noted that in Fig. 3A, needle-like sulfur was grown from the carbon nanotube surface. It is thought that the small solid sulfur particles formed on the active sites inside the MWNTs were rapidly transported by condensed water from the inner tubule to the tip and then along the outer surface of tube, as an homogeneous sulfur film. The sulfur film formed underwent nucleation into larger particles probably on the surface defects of the tubes leading to the very large solid sulfur spheres observed. The SEM image (Fig. 3B) clearly shows the sulfur flowing away from the tube tip and trickling down along the outer surface of the tube. According to this sulfur nucleation mode, one should expect the continuous cleaning of the NiS_2 active phase located inside the MWNTs, allowing the maintenance of the initial desulfurization activity.

The improvement in the storage capacity of the catalyst was attributed to the increase in the free volume of the MWNT-based catalyst, which remained available for sulfur storage during the reaction, when compared to the grain size SiC-based catalyst. The void volume outside the MWNTs

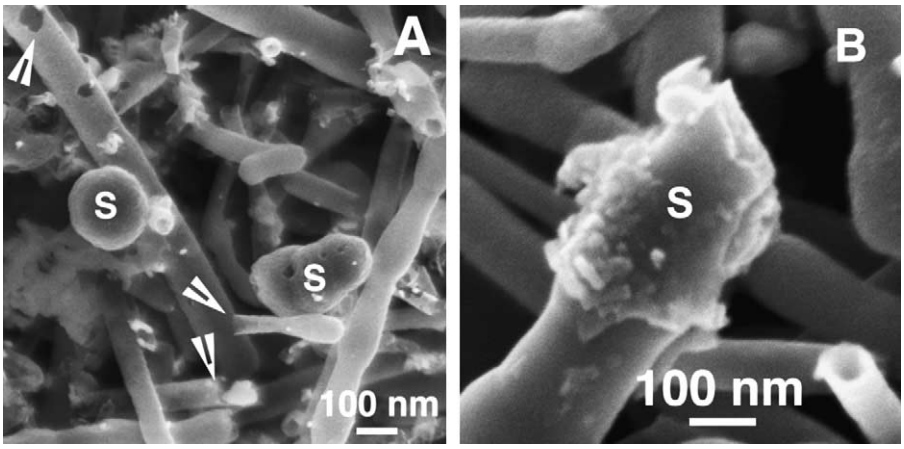

Fig. 3. SEM micrographs evidencing the location of the solid sulfur on the NiS_2/MWNTs catalyst containing 180 wt.% of sulfur after desulfurization test at 60 °C. (A) Low-magnification SEM image of the NiS_2/MWNTs catalyst after reaction with a sulfur loading of 180 wt.%. (B) High-magnification SEM image showing the solid sulfur trickle-down from the tube tip.

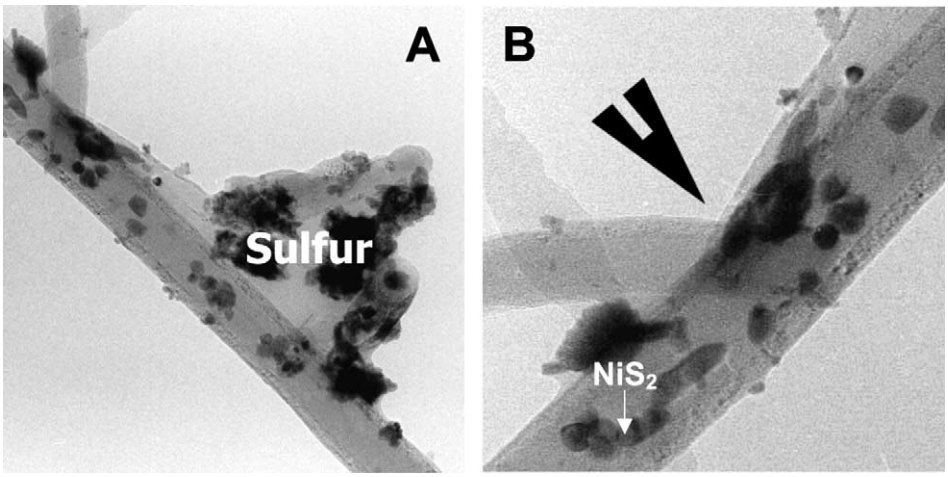

Fig. 4. TEM micrographs of the NiS_2/MWNT catalyst after reaction. (A) Low-magnification TEM image showing the solid sulfur aggregates located on the outer surface of the carbon nanotube. (B) High-magnification TEM image evidence the presence of a low wetting angle between the solid sulfur and the carbon nanotube outer surface.

being much larger than that of SiC grains, larger amounts of solid sulfur could also be stored in the external void volume, where no NiS_2 particles are located, without deactivation by active site encapsulation.

TEM image of the catalyst after reaction shows the presence of a large amount of sulfur on the outer surface of the MWNT (Fig. 4A) whereas almost no sulfur was observed inside the inner channel. The low wetting angle between the solid sulfur aggregates and the outer surface of the tube also indicates the hydrophobic character of the surface as advanced above (Fig. 4B). Note that almost no sulfur was observed inside the carbon nanotube channel which indicate that the rate of the sulfur removal from the inner channel onto the surface was relatively high.

4. Conclusion

A NiS_2-based catalyst encapsulated inside MWNTs was successfully used for the trickle-bed oxidation of H_2S into elemental sulfur at 60 °C. The use of MWNTs led to a significant increase in the overall catalytic performance, both in terms of desulfurization activity and resistance to the solid sulfur deposition onto the material as compared to the reference catalyst supported on macroscopic SiC grains. On the MWNT-based catalyst, a phenomenon of conveyor belt from the inner tubule, where the active phase is located, to the external graphene sheet of MWNTs, which are free of active phase, has been advanced to explain the maintenance of a high desulfurization activity without any deactivation by encapsulation with solid sulfur. The high capacity of solid sulfur storage on the MWNT-based catalyst compared to that of macroscopic SiC grains was thus attributed to the large void volume outside the MWNTs, available for the sulfur storage, when compared to the void volume outside the SiC grains.

References

[1] S. Iijima, Nat. Lond. 354 (1991) 56.
[2] T.W. Ebbesen, Carbon Nanotubes: Preparation and Properties, CRC Press, Boca Raton, FL, 1997.
[3] M. Terrones, W. Kuang Hsu, H.W. Kroto, D.R.W. Walton, Top. Curr. Chem. 199 (1999) 189.
[4] P.M. Ayajan, Chem. Rev. 99 (1999) 1787.
[5] N.M. Rodriguez, M.S. Kim, R.T.K. Baker, J. Phys. Chem. 98 (1994) 1310.
[6] A. Chambers, T. Nemes, N.M. Rodriguez, R.T.K. Baker, J. Phys. Chem. B 102 (1998) 2251.
[7] C. Park, R.T.K. Baker, J. Phys. Chem. B 102 (1998) 5168.
[8] F. Salman, C. Park, R.T.K. Baker, Catal. Today 53 (1999) 385.
[9] K.P. de Jong, J.W. Geus, Catal. Rev.-Sci. Eng. 42 (4) (2000) 481.
[10] C. Pham-Huu, N. Keller, L.J. Charbonnière, R. Ziessel, M.J. Ledoux, Chem. Commun. (2000) 1871.
[11] E.S. Steigerwalt, G.A. Deluga, C.M. Lukehart, J. Phys. Chem. B 106 (2002) 760.
[12] C. Pham-Huu, N. Keller, M.J. Ledoux, J. Catal. 200 (2) (2001) 400.
[13] M.J. Ledoux, R. Vieira, C. Pham-Huu, N. Keller, J. Catal. 216 (2003) 333.
[14] Sulphur 252 (1997).
[15] Sulphur 231 (1994).
[16] J. Wieckowska, Catal. Today 24 (1995) 405.
[17] Sulphur 257 (1998).
[18] A. Piéplu, O. Saur, J.-C. Lavalley, O. Legendre, C. Nedez, Catal. Rev.-Sci. Eng. 43 (4) (1998) 409.
[19] N. Keller, C. Pham-Huu, C. Crouzet, M.J. Ledoux, S. Savin-Poncet, J.-B. Nougayrède, J. Bousquet, Catal. Today 53 (4) (1999) 535.
[20] M.J. Ledoux, C. Pham-Huu, N. Keller, J.-B. Nougayrède, S. Savin-Poncet, J. Bousquet Catal. Today 61 (2000) 157.
[21] N. Keller, C. Pham-Huu, M.J. Ledoux, Appl. Catal. A: Gen. 217 (2001) 205.
[22] Y. Gogotsi, J.A. Libera, A.G. Yazicioglu, C.M. Megaridis, in: A.M. Rao (Ed.), MRS Symposium Proceedings on Nanotubes and Related Materials, vol. 633, Pittsburgh, PA, 2001, pp. A7.4.1–4.6.
[23] T.W. Ebbesen, Acc. Chem. Res. 31 (1998) 558.
[24] (a) J.A. Libera, Y. Gogotsi, Carbon 39 (2001) 1307;
(b) Y. Gogotsi, N. Naguib, J.A. Libera, Chem. Phys. Lett. 365 (2002) 354.

[25] C. Pham-Huu, N. Keller, C. Estournès, G. Ehret, M.J. Ledoux, Chem. Commun. (2002) 954.
[26] N. Keller, C. Pham-Huu, C. Estournès, M.J. Ledoux, Appl. Catal. A: Gen. 234 (2002) 193.
[27] M. Steijns, F. Derks, A. Verloop, P. Mars, J. Catal. 42 (1976) 87.
[28] J. Klein, H.D. Henning, Fuel 63 (1984) 1064.
[29] M.J. Ledoux, C. Pham-Huu, CaTTech 5 (4) (2001) 226.
[30] B.W. Gamson, R.H. Elkins, Chem. Eng. Prod. 49 (1953) 203.